Journal of Control, Automation and Electrical Systems (2019) 30:1116–1125
https://doi.org/10.1007/s40313-019-00527-1

Transient Stability of Power Systems Under High Penetrations of Wind Power Generation

Alexandre P. Sohn[1] · **Maurício B. de C. Salles**[2] · **Luís F. C. Alberto**[1]

Received: 7 May 2019 / Revised: 20 August 2019 / Accepted: 24 September 2019 / Published online: 3 October 2019

Abstract
This paper investigates the impact of high levels of penetration of wind power generation in the problem of transient stability of power systems. The investigation takes into account the stability issues related to the disconnection of wind power plants due to violation of voltage limits defined by the low-voltage ride-through curve. Different levels of penetration are investigated, starting at 10.59% for wind power plants based on types 1, 2, 3 and 4 wind turbine generators, until 75.24% for those based on type 3. Simulation results show that the secure power system operation can be maintained in most of the situations, from the point of view of transient stability, for the crescent penetration of wind power plants.

Keywords Low-voltage ride-through · Transient stability · Wind power generation

1 Introduction

The size of wind power plants has significantly increased in recent years, and substantial capacity additions are expected for the next years (IEA 2016). Differently from conventional power plants, in which synchronous generators are generally employed, wind power plants often employ induction generators or generators that are fully connected to the grid via power converters (Li and Chen 2008; Mahela and Shaik 2016). Once the dynamics of these plants are different from each other, their impacts on transient stability have to be investigated to ensure secure operation of power systems.

With different types of generators connected to the grid, including connections via power converters, not only the conventional loss of synchronism of synchronous generators (Kundur et al. 2004) needs to be investigated. Induction generators or generators that are fully connected to the grid via power converters usually do not have problems with synchronism due to the fast response of the typical phase-locked loop algorithms, but turbines can stall or accelerate, indicating the necessity of checking rotor speed stability (Samuelsson and Lindahl 2005). Moreover, wind power plants are more sensitive to disconnection due to low voltage profiles, as compared to synchronous generators. Consequently, the problem of voltage stability and the stability issues related to the disconnection of wind power plants due to low voltage limits violation are relevant for the transient stability analysis (Howlader and Senjyu 2016).

Several authors have investigated the impact of wind power plants on stability of power systems. In Slootweg and Kling (2003), the stability of a wind power plant was investigated in two test systems. It was observed that power system oscillations were directly affected by the wind turbine generator (WTG) type and its penetration. In Anaya-Lara et al. (2006), it was verified that the fixed-speed wind turbines could contribute to the oscillation damping. The results also showed that wind power plants based on doubly fed induction generators (DFIGs) exhibited superior transient performance as compared to those based on fixed-speed wind turbines. In Muljadi et al. (2007), it was concluded that a wind power plant based on DFIGs with low-voltage ride-through (LVRT) capability could be introduced in weak grids

The authors would like to thank Professor Rodrigo Andrade Ramos for helpful discussions and the availability of the PSS®E software. This study was financed in part by the Coordenação de Aperfeiçoamento de Pessoal de Nível Superior (CAPES) - Finance Code 001, in part by Brazilian National Research Council (CNPq) under the Grant 308067/2017-7 and in part by the National Institute of Science and Technology (INCT) project under the Grant 2014/50851-0 of São Paulo Paulo Research Foundation (FAPESP).

✉ Alexandre P. Sohn
alexandresohn@usp.br

[1] Department of Electrical Engineering, University of São Paulo, São Carlos, Brazil

[2] Department of Energy and Automation Engineering, University of São Paulo, São Paulo, Brazil

without compromising transient stability. In Muljadi et al. (2009), an equivalent wind power plant based on DFIGs is added to a small test system and then replaced by a conventional synchronous generator. From the transient performances observed, it was concluded that when the wind power plant is considered, a more stabilizing impact on power system is achieved. In Gautam et al. (2009), beneficial and adverse impacts of increased penetration of wind power plants on transient and small signal stability performances were observed. In Vittal et al. (2012), it was shown how the reactive power support from DFIG wind generation is critical to transient stability. It was verified that oscillations were damped more quickly when a terminal voltage control mode was used. In Edrah et al. (2015), impacts on rotor angle stability of synchronous generators considering a penetration of 27% of wind generation from WTGs based on DFIGs were investigated. From the results obtained by the authors, the main conclusion is that replacing synchronous generators by a wind power plant without appropriate control strategies, the rotor angle stability of synchronous generators can be negatively affected. With appropriate control schemes, the wind power plant becomes able to damp power system oscillations.

In this paper, we extend the existing analysis by investigating the impact of different types and levels of penetration of wind power generation in transient stability. Once wind power plants are subject to disconnection due to violation of operational limits, according to the LVRT curve, this problem is also considered here. The LVRT curve determines conditions for uninterrupted operation of the wind power plant even at low voltage levels. In other words, this curve establishes that the wind power plant must stay connected to the point of common coupling (PCC) under low voltage levels for specific time intervals. If the voltage at the PCC violates the voltage limits of the curve, then the wind power plant can be disconnected from the grid (Mohseni and Islam 2012; Singh and Singh 2009).

In this paper, the violation of the aforementioned curve will indicate the vulnerability of the wind power plant to be disconnected by protection schemes in the study of transient stability. If the voltage limits are violated, we will consider the system unsafe and critical clearing times (CCTs) will be calculated to avoid violation of these limits. The LVRT curve proposed by the Federal Energy Regulatory Commission for the USA is considered here (FERC 2005). Although this curve was chosen, many other countries have their own curve (Ackermann 2012; Iov et al. 2007).

The main contributions of this paper are to identify the mechanism that causes instability in a mixed-generation network composed of synchronous generators and wind power plants based on the four major types of WTGs and to check how the transient stability is affected by increasing levels of penetration of wind power plants, determining appropriate

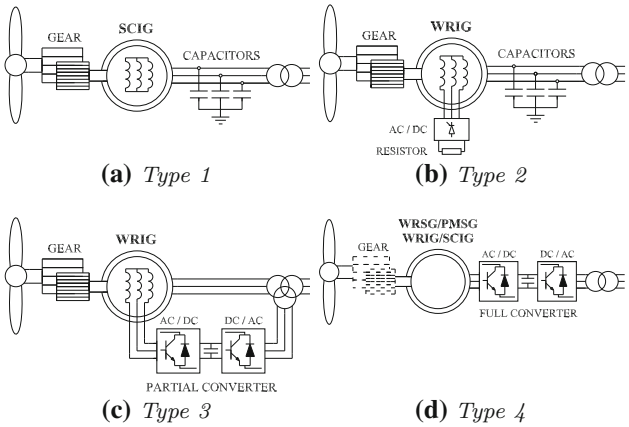

Fig. 1 Typical wind turbine generator topologies

CCTs. Differently from the existing analysis in the literature, much higher penetrations in the electrical system are now considered in a multi-machine test system. Also, the aforementioned stability problems, including consequences of eventual disconnections of wind power plants, are now assessed together for complete models of generating plants. In this sense, all these aspects are brought together in the same paper, providing to readers an overview of the transient stability phenomena involved in a renewable energy system.

The body of this paper is organized in six sections. After this introduction, Sect. 2 discusses the different topologies of WTGs. Section 3 summarizes the WTGs and synchronous generators models. Section 4 describes the equivalent wind power plants models, the test system and the penetration cases under study. Section 5 exhibits the results and analysis. Finally, Sect. 6 presents the discussion and the main conclusions of this work.

2 Wind Turbine Generator Topologies

Four WTG topologies are prevalent in the market (Ackermann 2012; Vittal and Ayyanar 2013; Yaramasu and Wu 2017). They can be classified into fixed-speed (type 1), limited-variable-speed (type 2) or variable-speed (types 3 and 4) wind turbines. The stall, pitch or active stall control can be applied to type 1. For the other topologies, normally the pitch control is used. Each typical topology is depicted in Fig. 1.

The Type 1 topology is equipped with a squirrel cage induction generator (SCIG) directly connected to the grid via a transformer. A gearbox is necessary to match the low turbine speed to the high generator speed. In this topology, wind fluctuations are directly converted into mechanical and electrical fluctuations. Evidently, oscillations from the grid have immediate effects on the WTG performance. Once SCIG draws large amounts of reactive power, a capacitor bank is

necessary for compensation. Here, the controllability of the active and reactive powers, besides the voltage, is relatively poor.

The Type 2 topology is equipped with a wound rotor induction generator (WRIG) and a variable additional rotor resistance controlled by power electronics. The idea is to control the slip and then to improve the wind power extraction and the power output.

The Type 3 topology is equipped with a WRIG and a partial-scale back-to-back converter. This configuration is also known as DFIG (Abad et al. 2011). The stator of the generator is directly connected to the grid via a transformer. The back-to-back converter connects the generator rotor circuits to the grid, and it is rated around 30% of the generator nominal power. This configuration is able to provide reactive power support and hence contributes to the voltage control. Indeed, the active and reactive power can be independently adjusted in a quick manner, providing a grid connection smoother than that offered by the types 1 and 2 WTGs.

The Type 4 topology can be equipped with different generators. Generators with multipole configuration, permanent magnet synchronous generator (PMSG) and wound rotor synchronous generator (WRSG), can be constructed without gearbox or with low-speed transformation. The generator is connected to the grid via a full-scale converter and a transformer (Maswood and Tafti 2019). The converter decouples the dynamics of the generator from the dynamics of the grid, allowing a wide speed range for the generator and active and reactive power regulations, including voltage control. Thus, the grid connection is improved with this type of WTG (Michalke 2008).

3 Wind Turbine Generator and Synchronous Generator Models

The WTGs are modeled by means of generic models. Vendor-specific models of wind turbines are able to provide more accurate representation; however, they are often unavailable or difficult to obtain. Generic models are nonproprietary models that were created to overcome these difficulties and to allow several manufacturers to represent their equipments by an adequate parametrization. Moreover, these models can be implemented in different positive-sequence simulation programs for stability, planning and interconnection studies at the bulk power system level (Ellis et al. 2011a, b).

Each generic model is interconnected by several modules, as can be seen in Fig. 2a–d. Type 1 is composed of the generator (WT1G), wind turbine (WT12T) and pseudogovernor (WT12A) modules. Type 2 is composed of the generator (WT2G), wind turbine (WT12T), pseudogovernor (WT12A) and rotor resistance control (WT2E) modules. Type 3 is composed of the generator/converter (WT3G), converter control

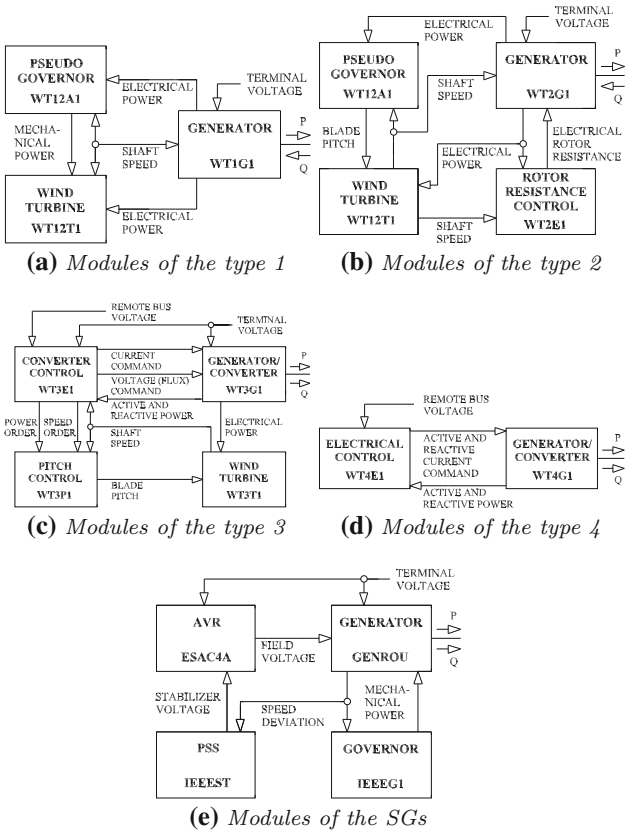

Fig. 2 Modules of the wind turbine generators and synchronous generators

(WT3E), wind turbine (WT3T) and pitch control (WT3P) modules. Type 4 is composed of the generator/converter (WT4E) and electrical control (WT 4E) modules.

Once each generic model is composed of different modules, the detailed description of each module is not possible due to the limited space available. However, a detailed background about each generic model can be found for implementation in Siemens (2019) and ESIG (2019), as well as all parameters necessary for the simulations performed in this paper.

With respect to the synchronous generators, each model of this type of machine (GENROU) is equipped with an automatic voltage regulator (ESAC4A), a power system stabilizer (IEEEST) and a governor (IEEEG1), as can be seen in Fig. 2. Each module of this model can be found in Canizares et al. (2015), as well as the parameters necessary for the simulations performed in this paper.

As can be seen in Fig. 2, no protection system is modeled. It is emphasized that due to the available limited space, the diagram blocks of each complete model of the wind power plants and synchronous generators, as well as all parameters used in the simulations, are not presented in this paper, but all of them can be found in Siemens (2019), ESIG (2019) and Canizares et al. (2015).

Table 1 Wind turbine generators used in generic models

Manufacturer	Model	Type	Individual power (MW)
Mitsubishi	MWT-1000A	1	1.0
Vestas	V80	2	1.8
General electric	1.5	3	1.5
General electric	2.5	4	2.5

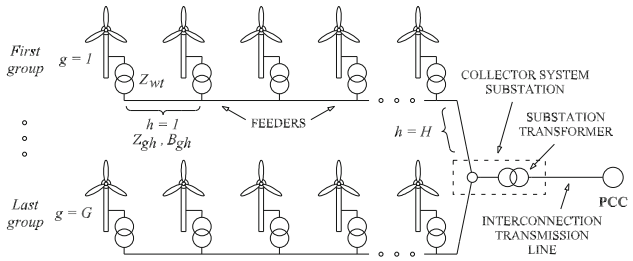

Fig. 3 Wind power plant topology

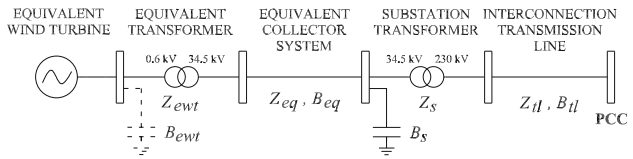

Fig. 4 Equivalent wind power plant

4 Wind Power Plant Model and Test System

For bulk power systems, the operator is not concerned with the internal details of the plant, but how it impacts the transmission system at the PCC (Ackermann 2012). In this paper, we employ an equivalent aggregated model to represent the wind power plant. An analytical approach was developed in Muljadi et al. (2006) to obtain equivalent parameters and models of wind power plants.

The equivalent model of a wind power plant is based on a simplified single-machine equivalent system that takes into account hundreds of megawatt-scale WTGs of the same type interconnected by their step-up transformers and feeders, a substation and a transmission line. The equivalent WTG expresses the sum of all WTG individual powers, and each type of WTG is based on a manufacturer model according to Table 1. The original topology of the wind power plant and the derived equivalent are depicted in Figs. 3 and 4.

All assumptions adopted to calculate the equivalent parameters of the wind power plants are described in Muljadi et al. (2006). The parameters of the equivalent model of Fig. 4 are calculated by

$$Z_{\mathrm{ewt}} = R_{\mathrm{ewt}} + jX_{\mathrm{ewt}} = \frac{Z_{\mathrm{wt}}}{N} \tag{1}$$

$$Z_{\mathrm{eq}} = R_{\mathrm{eq}} + jX_{\mathrm{eq}} = \frac{\sum_{g=1}^{G}\sum_{h=1}^{H} h^2 Z_{\mathrm{gh}}}{N^2} \tag{2}$$

$$B_{\mathrm{eq}} = \sum_{g=1}^{G}\sum_{h=1}^{H} B_{\mathrm{gh}} \tag{3}$$

where Z_{wt} is the impedance of the transformer of each individual WTG, Z_{ewt} is the impedance of the equivalent transformer, Z_{gh} and B_{gh} are the series impedance and the total parallel susceptance of the π model for each branch, Z_{eq} and B_{eq} are the series impedance and the total parallel susceptance of the equivalent collector system, G is the total number of groups of WTGs, H is the total number of branches for each group of WTGs and N is the total number of WTGs in the wind power plants.

The parameter Z_{s} is the impedance of the substation transformer and Z_{tl} and B_{tl}, the series impedance and the total susceptance of the π model of the transmission line. Each complete group of WTGs is composed of 60 WTGs. The last group varies according to the total power of the wind power plant. The terminal capacitor is employed only for equivalent wind power plants of types 1 and 2. The substation capacitor is included in all wind power plants to maintain the voltage at the buses within the equivalent wind power plant between 0.97 pu and 1.03 pu and the voltage at the other buses, including the PCCs, as close as possible to those of the base case.

In order to assess the transient stability of a power system under high penetrations of wind power generation, the New England Test System was chosen for study (Pai 1989). It has 39 buses, ten synchronous generators (6140.7 MW / 1264.3 Mvar), 19 loads (6097.1 MW / 1408.7 Mvar) and 46 transmission lines. The visualization of this system is depicted in Fig. 5.

Each synchronous generator and its transformer are replaced by an equivalent wind power plant according to Table 2 to increase the penetration of wind power plants. For case 1, only the synchronous generator G3 is replaced by a wind power plant. For this case, the impacts of wind power plants based on types 1, 2, 3 and 4 WTGs are analyzed and compared. For other penetration cases, only wind power plants based on the type 3 WTGs are considered, once they show a significant participation in the market today and certainly will be among the most common configurations of WTGs in the future (FTI 2018).

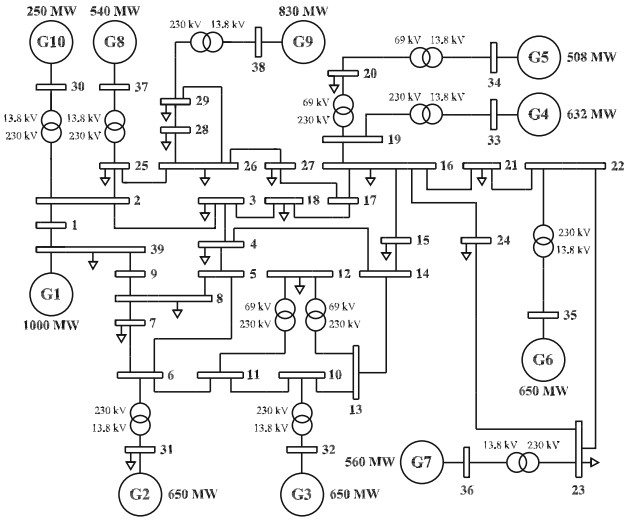

Fig. 5 New England test system

5 Results and Analysis

The PSS®E software was chosen for time-domain simulations considering: (1) 100 MVA and 60 Hz bases, (2) for the pre-fault system, the full Newton–Raphson method was used to calculate the power flow, (3) the modified Euler method was used to carry out the dynamic simulations, with a time step of 0.00833 s, (4) CCTs are computed by repetitive simulations, (5) each load of the test system was modeled by a constant admittance in dynamic simulations, (6) the disturbance, applied to several buses of the test system, corresponds to a solid three-phase-to-ground fault, (7) the wind power plants based on the types 1 and 2 WTGs do not control any bus voltage, while the synchronous generators and the wind power plants based on the types 3 and 4 WTGs control the terminal voltage and (8) all simulations were performed for 6 s with the fault applied at 1 s.

The synchronism among conventional synchronous generators, the rotor speed stability of induction generators and stability issues related to the disconnection of wind power plants due to violation of the LVRT curve are assessed together considering several faults applied to the test system of Fig. 5. The results and analysis are separated in two subsections. In Sect. 5.1, a brief analysis of dynamics of the base case and case 1 is presented, comparing the wind power plants based on the types 1, 2, 3 and 4 WTGs with the dynamics of the synchronous generator G3 of the base case. The CCTs, for several faults, are computed and compared among the generating plants in Table 3. In Sect. 5.2, the analysis is extended to all cases of Table 2 investigating the impact of increasing penetration of wind power plants based on the type 3 WTGs, showing the CCTs in Table 4.

5.1 Comparing Different Types of Wind Power Plants

As already mentioned in Table 2, for case 1, only the synchronous generator G3 is replaced by an equivalent wind power plant. First of all, what occurs when a 250 ms fault is applied to bus 14 of the test system in Fig. 5 is verified. For this disturbance, (1) the synchronous generators remained in synchronism, (2) the equivalent WTGs did not stall neither accelerate indefinitely, (3) the voltage stability was ensured in the sense that all voltages returned to values close to nominal ones after fault clearing and (4) only the wind power plants based on the types 1 and 2 WTGs violated the LVRT curve. The intentional disconnection of these wind power plants did not compromise the transient stability of the power system, since the variables returned to values close to nominal ones after disconnection. It is emphasized that the trip of generating plants due to under-frequency protection schemes was not considered in these studies.

As well known, the reactive power supplied by the generating plants is essential to keep the voltages of the power system in adequate levels. The reactive power flow behavior at the PCC is depicted in Fig. 6. Negative values indicate that the reactive power flows from substation to PCC (injecting reactive power to the grid), while positive values flow from PCC to substation (absorbing reactive power from the grid). In the pre-fault system, the reactive power flow is different among the different types of generating plants, since the impedance

Table 2 Penetrations of wind power generation

Case	Replaced synchronous generators	Wind power (MW)
Base	–	0 (0 %)
1	G3	650 (10.59 %)
2	G3, G4	1282 (20.88 %)
3	G3, G4, G5	1790 (29.15 %)
4	G3, G4, G5, G6	2440 (39.73 %)
5	G3, G4, G5, G6, G7	3000 (48.85 %)
6	G3, G4, G5, G6, G7, G8	3540 (57.65 %)
7	G3, G4, G5, G6, G7, G8, G9	4370 (71.16 %)
8	G3, G4, G5, G6, G7, G8, G9, G10	4620 (75.24 %)

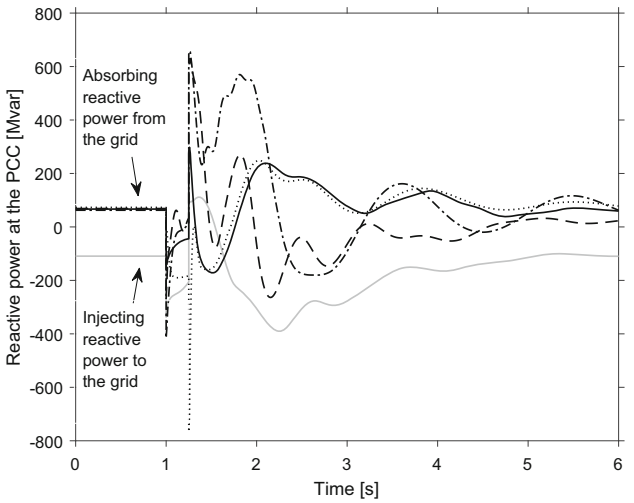

Fig. 6 Reactive power at the PCC: synchronous generator G3 (solid gray), type 1 (dash dot), type 2 (dashed), type 3 (solid), type 4 (dotted)

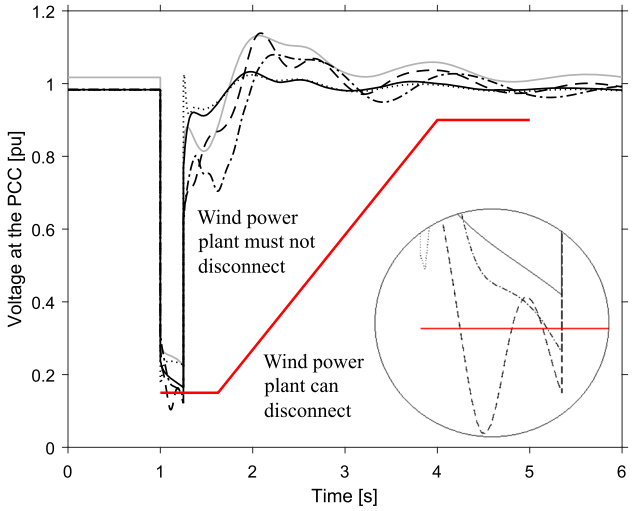

Fig. 7 Voltage at the PCC: synchronous generator G3 (solid gray), type 1 (dash dot), type 2 (dashed), type 3 (solid), type 4 (dotted), LVRT curve (thick)

and capacitance of the equivalent wind power plants are different from those of the transformer of the synchronous generator. As can be seen in Fig. 6, the wind power plants drain reactive power from the grid while the synchronous generator injects reactive power before the occurrence of the fault.

The reactive power provided by the capacitors could be increased in order to equalize the reactive power at the PCC among all generating plants, but it was considered the smallest values which are sufficient to maintain the internal voltages of the equivalent wind power plants as close as possible to 1 pu and the voltage at the PCC close to the value of the base case.

The wind power plants based on the types 3 and 4 WTGs and the synchronous generator are configured to control the terminal voltage. In this sense, the reactive power regulation is improved in these generating plants. The highest reactive power support during the fault is achieved by the synchronous generator. Although the wind power plants based on the types 1 and 2 WTGs are able to provide some reactive power during the fault, they are not able to keep the reactive power supply in levels as high as the ones provided by synchronous generator and the wind power plants based on the types 3 and 4.

The voltage behavior at the PCC is depicted in Fig. 7. Severe voltage sags can be observed, once the fault is electrically close to the PCC. Comparing the response of the wind power plants, we observe that those based on the types 3 and 4 WTGs keep the voltages at the highest levels during the fault and present the best voltage regulation in the post-fault system. Due to the lack of reactive power support, only the wind power plants based on the types 1 and 2 WTGs violate the voltage limits of the LVRT curve, as evidenced in the detail of Fig. 7. Consequently, these generating plants are subject to disconnection and the system is considered unsafe in this situation.

Table 3 shows the CCTs for the base case and case 1, considering the four types of wind power plants. These times are represented in milliseconds and classified according to: (1) when the CCT is greater or equal to the CCT of the base case, this time is identified by the symbol •, (2) when the CCT is smaller than the CCT of the base case, this time is identified by the symbol ⋆ and (3) when the CCT guarantees no violation of the LVRT curve, this time is identified by the symbol ◇.

The LVRT curve is considered in all scenarios; however, only in some scenarios, the voltage limits of the curve are violated. If this curve is not violated, then the registered CCTs are the maximum time intervals in which the synchronous generators remain in synchronism and the WTGs remain stable from the point of view of rotor speed stability and voltage stability. In other words, for all computed CCTs of Table 3, both rotor speed stability and voltage stability are ensured for the wind power plants while the synchronous generators remain in synchronism. For any clearing time greater than the registered value, the synchronous generator that loses synchronism is indicated. Considering the LVRT curve violation, the respective PCC in which the LVRT curve is violated is indicated, as well as the maximum time interval in which the LVRT curve is not violated.

When the synchronous generator G3 is replaced by wind power plants based on types 3 and 4 WTGs, greater CCTs are achieved. As can be seen in Table 3, all CCTs are greater or equal than those of the base case. The reactive power support, the active and reactive power controls, the fast pitch control (rate between $\pm 10°$/s) and the decoupling between

Table 3 Critical clearing times (ms) for the base case and for case 1

Bus fault	Base case	Type 1	Type 2	Type 3	Type 4
31	250 G2	⋆233 G2	⋆225 G2	•250 G2	•250 G2
6	258 G2	⋆250 G2	⋆241 G2	•275 G2	•266 G2
		◇91 10	◇50 10	◇258 10	◇8.33 10
5	275 G2, G3	⋆258 G2	⋆258 G2	•291 G2	•291 G2
		◇250 10	◇66 10		
10	250 G3	•366 G2	•375 G2	•408 G2	•416 G2
		◇8.33 10	◇8.33 10	◇8.33 10	◇8.33 10
13	283 G3	•383 G2	•391 G2	•425 G2	•458 G2
		◇8.33 10	◇8.33 10	◇8.33 10	◇8.33 10
4	308 G5	•308 G2	•316 G2	•350 G5	•400 G1
			◇91 10		
14	316 G5	•333 G2	•341 G2	•375 G5	•416 G5
		◇216 10	◇66 10	◇308 10	
3	308 G5	⋆275 G5	⋆266 G2, G5	•316 G5	•325 G2
18	308 G5	⋆275 G5	⋆258 G2	•308 G5	•316 G1
27	241 G9	•241 G9	•241 G9	•241 G9	•250 G9

the machine and the grid are the main reasons that justify the better results.

When we consider CCTs to avoid violation of the LVRT curve, these times are smaller than those related to the synchronous generators. In several situations, these times are very small. For example, observing the CCTs for the faults applied to buses 10 and 13, the wind power plants connected to these buses are very sensitive to disconnection. In these cases, the CCT 8.33 ms indicates that the violation of the LVRT curve occurs immediately after the fault occurrence.

For all cases where the LVRT curve was violated, i.e., the CCT for avoiding LVRT curve violation is smaller than the CCT to avoid loss of synchronism of synchronous generators, the wind power plant was intentionally disconnected to verify the impacts on the power system. For most cases, the disconnection of the wind power plant did not compromise the transient stability of the power system, since the variables returned to values close to nominal ones after disconnection. Obviously, the power system is considered unsafe if a large amount of power can be lost. Only for the fault on bus 6, the intentional wind power plant disconnection caused the loss of synchronism among the synchronous generators. Since the synchronous generator G2 is closer to bus 6, this is the first unit to lose the synchronism. This case is an example that the disconnection of a wind power plant can disrupt a cascade disconnection of other generating plants.

5.2 Impacts of Penetrations in Critical Clearing Times

In order to investigate high penetrations of wind power generation in the test system of Fig. 5, Table 4 shows the CCTs obtained for all cases presented in Table 2, considering only wind power plants based on type 3 WTGs. The formatting of Table 4 follows the same pattern of Table 3 in Sect. 5.1. All considerations of sixth and seventh paragraphs of Sect. 5.1 are also applicable to Table 4.

From Table 2, the synchronous generator G2 is never replaced by a wind power plant. From Fig. 5, buses 31 and 6 are the ones closest to the unit G2. Due to these aspects, we verify in Table 4 that when a fault is applied to these buses, the unit G2 is the one that loses the synchronism in all cases. In other words, the unit G2 loses the synchronism because it is the one closest to these faults. Investigating all faults for all cases, it is possible to assert that the synchronous generator that loses synchronism is the one closest to the bus fault. This dynamic behavior is usually expected to occur in most power systems, independent of the insertion of wind generation. However, with the presence of wind power plants close to the bus fault, the LVRT curve violation can occur and, therefore, an eventual disconnection becomes possible. In this context, not only the problem of synchronism should be considered, but also the stability issues related to the disconnection of wind power plants due to violation of voltage limits.

Table 4 indicates that the CCTs for most of situations are in general greater than or equal to the CCT of the base case when the wind power generation is present. As can be seen, most of the CCTs are indicated by the symbol •. Let's compare the base case and case 1 for the faults applied to buses 10 and 13. In the base case, the CCTs correspond to 250 ms and 283 ms, respectively. When we consider a wind power plant, these times increase to 408 ms and 425 ms, respectively. Actually, when the synchronous generator G3

Table 4 Critical clearing times (ms) for all cases

Bus fault	Base case	Case 1	Case 2	Case 3	Case 4	Case 5	Case 6	Case 7	Case 8
31	250 G2	•250 G2	•250 G2	•250 G2	⋆241 G2	⋆241 G2	⋆241 G2	⋆241 G2	⋆241 G2
6	258 G2	•275 G2	•266 G2	•266 G2	•266 G2	•258 G2	•258 G2	•258 G2	⋆250 G2
		◇258 10							
5	275 G2, G3	•291 G2	•283 G2	•283 G2	•275 G2	•275 G2	•275 G2	⋆266 G2	⋆250 G2
10	250 G3	•408 G2	•408 G2	•400 G2	•391 G2	•383 G2	•383 G2	•375 G2	•341 G2
		◇8.33 10	◇8.33 10	◇8.33 10	◇8.33 10	◇8.33 10	◇8.33 10	◇8.33 10	◇8.33 10
13	283 G3	•425 G2	•425 G2	•416 G2	•408 G2	•391 G2	•391 G2	•383 G2	•341 G2
		◇8.33 10	◇8.33 10	◇8.33 10	◇8.33 10	◇8.33 10	◇8.33 10	◇8.33 10	◇8.33 10
4	308 G5	•350 G5	•350 G2	•341 G2	•333 G2	•325 G2	•325 G2	•316 G2	⋆283 G2
14	316 G5	•375 G5	•400 G2	•391 G2	•383 G2	•375 G2	•375 G2	•366 G2	•316 G2
		◇308 10	◇308 10	◇308 10	◇308 10	◇308 10	◇300 10	◇308 10	◇266 10
3	308 G5	•316 G5	•333 G5	•333 G9	•325 G9	•308 G9	⋆283 G9	•333 G2	⋆283 G2
									◇266 2
18	308 G5	•308 G5	•325 G5	•333 G9	•333 G9	•308 G9	⋆291 G9	•383 G2	⋆300 G2
27	241 G9	•241 G9	•241 G9	•241 G9	⋆233 G9	⋆225 G9	⋆225 G9	•575 G2	•383 G2

is replaced by a wind power plant, we observe an increase in the CCTs, since with the substitution by a wind power plant, the synchronous generator G3 is no longer present. As can be seen, the synchronous generator that loses synchronism changes to unit G2.

Another example for this type of situation refers to fault applied to buses 18 and 27, considering cases 6 and 7. The CCT changes from 291 ms in case 6 to 383 ms in case 7 for the fault on bus 18 and changes from 225 ms in case 6 to 575 ms in case 7 for the fault on bus 27. In both situations, the synchronous generator that loses the synchronism changes, since the synchronous generator that loses the synchronism corresponds to unit G9 in case 6 and to unit G2 in case 7. In such situations, the CCT usually is increased.

Another important observation is related to the fact that the CCTs usually slightly decrease as the penetration of wind power generation increases, considering that the synchronous generator that loses synchronism remains the same. Once wind power plants based on type 3 WTGs are partially decoupled from the grid, these units do not contribute to the inertia of the system like the synchronous generators. In this sense, the total momentum of the system decreases as the wind power penetration increases. Since the inertial response of the synchronous generators is especially influenced in the first seconds, the CCTs become smaller. Modern WTGs are able to emulate inertia (and grid codes already require this behavior), but these studies are outside the scope of this work and will be considered as future work. That is, this scenario of reduction of CCT with increased penetration can still be reversed with the inertia emulation.

It is important to note that low voltage profiles are usually observed close to the faulted bus. Because of that, it is expected that the LVRT curve violation happens before the loss of synchronism among the synchronous generators when faults are applied close to the PCC. Particularly for the tested scenarios (faults applied to buses 10, 13 and 14), the LVRT curve was violated in the PCC represented by bus 10, even if up to eight synchronous generators were replaced by a wind power plant. For almost all other scenarios, the loss of synchronism was observed before the LVRT violation.

With respect to the CCTs related to the LVRT curve, one more time, it is visible that in some situations the wind power plant can be disconnected from the grid, since the CCTs related to the LVRT curve violation are generally smaller than those related to the rotor angle stability.

Considering the cases where the LVRT curve was violated, only for case 1 and for the fault on bus 6, the intentional disconnection of the wind power plant caused the loss of synchronism among the synchronous generators and the instability of the overall system.

6 Conclusions

This paper investigated the impact of penetration of wind power generation in the problem of transient stability of a power system composed of conventional synchronous generators and wind power plants. Different levels of penetrations of wind power plants based on the four major topologies of WTGs were considered and compared. Several simulations indicated that the dynamics of wind power plants are stable

and hardly ever a wind power plant becomes unstable due to rotor acceleration or due to a voltage instability phenomenon when the system is subjected to a large perturbation.

The best performance (greater CCTs) was obtained for the wind power plants based on the types 3 and 4 WTGs. Due to the decoupling between the dynamics of the rotor and the dynamics of the grid, the efficient pitch control, the reactive power support and the active and reactive power controls, the voltage recovery was improved and the power oscillations were reduced, positively impacting the power system transient stability.

However, for many cases of stable dynamics, wind power plants were subjected to very low levels of voltage and consequently subjected to disconnection by under-voltage protection schemes. In order to take into account the vulnerability of the system regarding the disconnection of a wind power plant, the LVRT curve was employed as a limit and CCTs were recalculated to avoid the violation of the LVRT curve. Considering the LVRT curve, the corresponding CCTs were generally small, showing that it is imperative to consider these limits to ensure secure operation of power systems with high penetration of wind power generation.

For the analyzed cases, when the loss of synchronism of other synchronous generator with the substitution of a synchronous generator by a wind power plant is observed, the CCT becomes always greater or remains equal to that of the previous case. It has also been observed that when the synchronous generator that loses synchronism remains the same as the wind power generation increases, the CCTs usually slightly decrease.

The main conclusion is that the secure power system operation can be maintained in most of the situations from the point of view of transient stability, for the crescent penetration of wind power plants, provided that the reactive support and appropriate active and reactive power controls are employed to avoid instability and the violation of the LVRT curve. Once these measures are taken, the transient stability margins can even be improved with high levels of wind power generation.

Therefore, this paper sheds light in the main issues that the power system operators and transmission planners are facing with the crescent penetration of wind power, regarding transient stability.

Appendix

The power flow data of Fig. 5 can be found in Pai (1989). The dynamic data of the governor model can be found by means of the Luc Gérin-Lajoie report in Canizares et al. (2015). For the IEEEG1 model, the original parameter $P_{\max}$ (9 pu) was modified to (11 pu) for all machines. The dynamic data of the synchronous generator, voltage regulator and power system stabilizer models can be found by means of the Ian Hiskens report in Canizares et al. (2015). For the unit G10, the original parameters T'_{qo} (0 s) and x'_q (0.008 pu) were modified. The first was modified to (0.1 s). Considering $x'_q > x'_d$ for round rotor generators, the second was modified to (0.032 pu). The subtransient parameters T''_{do} (0.05 s), T''_{qo} (0.035 s) and $x''_d = x''_q$ were considered for all machines and for all synchronous generators [G1 (0.004), G2 (0.05), G3 (0.045), G4 (0.035), G5 (0.089), G6 (0.04), G7 (0.044), G8 (0.045), G9 (0.045), G10 (0.025)] in per unit system.

Table 5 shows the data of equivalent collector system, transmission line, transformers and capacitors of Fig. 4. For each equivalent collector system, the following data were considered: feeders with R_{gh} (0.0002 pu), X_{gh} (0.0008 pu) and B_{gh} (0.0003 pu), regarding the topology of Fig. 3 with 60 individual WTGs per each complete group. Resistance and reactance values are represented in per unit system in the 100 MVA base, whereas the susceptance values are represented in Mvar. All per unit values found in Siemens (2019) and ESIG (2019) are described in machine MVA base. For N lumped machines, this base was multiplied by N.

Table 5 Data of equivalent collector system, transmission line, transformers and capacitors

Case	Type	WTs	R_{eq}	X_{eq}	B_{eq}	R_{tl}	X_{tl}	B_{tl}	X_{ewt}	X_{s}	B_{ewt}	B_{s}
1	A	650	0.00037	0.0015	190	0.0005	0.001	20	0.008	0.013	326	20
1	B	361	0.00068	0.0027	110	0.0005	0.001	20	0.008	0.013	333	20
1	C	434	0.00055	0.0022	130	0.0005	0.001	20	0.008	0.013	0	20
1	D	260	0.00088	0.0035	78	0.0005	0.001	20	0.008	0.013	0	20
2	C	422	0.00058	0.0023	130	0.0005	0.001	20	0.006	0.009	0	20
3	C	339	0.00068	0.0027	100	0.0006	0.0012	15	0.007	0.010	0	120
4	C	434	0.00055	0.0022	130	0.0005	0.001	20	0.005	0.010	0	100
5	C	374	0.00063	0.0025	110	0.0004	0.0011	18	0.010	0.014	0	80
6	C	360	0.00068	0.0027	110	0.0004	0.0013	16	0.010	0.015	0	80
7	C	554	0.00043	0.0017	170	0.0001	0.0008	10	0.006	0.010	0	130
8	C	167	0.0013	0.0053	50	0.009	0.004	40	0.007	0.010	0	40

References

Abad, G., López, J., Rodríguez, M. A., Marroyo, L., & Iwanski, G. (2011). *Doubly fed induction machine: Modeling and control for wind energy generation* (1st ed.). London: Wiley. https://doi.org/10.1002/9781118104965.

Ackermann, T. (Ed.). (2012). *Wind power in power systems* (2nd ed.). New York: Wiley. https://doi.org/10.1002/9781119941842.

Anaya-Lara, O., Hughes, F. M., Jenkins, N., & Strbac, G. (2006). Influence of windfarms on power system dynamic and transient stability. *Wind Engineering*, *30*(2), 107–127. https://doi.org/10.1260/030952406778055018.

Canizares, C., Fernandes, T., Geraldi, E, Jr., Gérin-Lajoie, L., Gibbard, M., Hiskens, I., et al. (2015). *Benchmark systems for small-signal stability analysis and control*. Technical report: IEEE Power and Energy Society.

Edrah, M., Lo, K. L., & Anaya-Lara, O. (2015). Impacts of high penetration of DFIG wind turbines on rotor angle stability of power systems. *IEEE Transactions on Sustainable Energy*, *6*(3), 759–766. https://doi.org/10.1109/TSTE.2015.2412176.

Ellis, A., Kazachkov, Y., Muljadi, E., Pourbeik, P., & Sanchez-Gasca, J. J. (2011a). Description and technical specifications for generic WTG models—a status report. In *2011 IEEE/PES power systems conference and exposition* (pp. 1–8). https://doi.org/10.1109/PSCE.2011.5772473.

Ellis, A., Muljadi, E., Sanchez-Gasca, J., & Kazachkov, Y. (2011b). Generic models for simulation of wind power plants in bulk system planning studies. In *2011 IEEE power and energy society general meeting* (pp. 1–8). https://doi.org/10.1109/PES.2011.6039844.

ESIG (2019) Energy systems integration group-generic models (individual turbines). https://www.esig.energy/wiki-main-page/generic-models-individual-turbines/#Structure.

FERC (2005). Interconnection for wind energy (docket no. rm05-4-000-order no. 661). FERC-Federal Energy Regulatory Commission, Washington, DC.

FTI. (2018). *Global wind market update-demand and supply 2017*. FTI consulting, Technical report .

Gautam, D., Vittal, V., & Harbour, T. (2009). Impact of increased penetration of dfig-based wind turbine generators on transient and small signal stability of power systems. *IEEE Transactions on Power Systems*, *24*(3), 1426–1434. https://doi.org/10.1109/TPWRS.2009.2021234.

Howlader, A. M., & Senjyu, T. (2016). A comprehensive review of low voltage ride through capability strategies for the wind energy conversion systems. *Renewable and Sustainable Energy Reviews*, *56*, 643–658.

IEA. (2016). World energy outlook.

Iov, F., Hansen, A. D., Sørensen, P., & Cutululis, N. A. (2007). Mapping of grid faults and grid codes. Technical report, Risø DTU National Laboratory for Sustainable Energy, Technical University of Denmark, Kongens Lyngby.

Kundur, P., Paserba, J., Ajjarapu, V., Andersson, G., Bose, A., Canizares, C., et al. (2004). Definition and classification of power system stability ieee/cigre joint task force on stability terms and definitions. *IEEE Transactions on Power Systems*, *19*(3), 1387–1401. https://doi.org/10.1109/TPWRS.2004.825981.

Li, H., & Chen, Z. (2008). Overview of different wind generator systems and their comparisons. *IET Renewable Power Generation*, *2*(2), 123–138. https://doi.org/10.1049/iet-rpg:20070044.

Mahela, O. P., & Shaik, A. G. (2016). Comprehensive overview of grid interfaced wind energy generation systems. *Renewable and Sustainable Energy Reviews*, *57*, 260–281. https://doi.org/10.1016/j.rser.2015.12.048.

Maswood, A. I., & Tafti, H. D. (2019). *Advanced multilevel converters and applications in grid integration* (1st ed.). New York: Wiley.

Michalke, G. (2008). Variable speed wind turbines-modelling, control, and impact on power systems. Ph.D. thesis, Darmstadt University of Technology, Darmstadt.

Mohseni, M., & Islam, S. M. (2012). Review of international grid codes for wind power integration: Diversity, technology and a case for global standard. *Renewable and Sustainable Energy Reviews*, *16*(6), 3876–3890. https://doi.org/10.1016/j.rser.2012.03.039.

Muljadi, E., Butterfield, C. P., Ellis, A., Mechenbier, J., Hochheimer, J., & Young, R., et al. (2006). Equivalencing the collector system of a large wind power plant. In *2006 IEEE power engineering society general meeting* (pp. 9). https://doi.org/10.1109/PES.2006.1708945.

Muljadi, E., Butterfield, C. P., Parsons, B., & Ellis, A. (2007). Effect of variable speed wind turbine generator on stability of a weak grid. *IEEE Transactions on Energy Conversion*, *22*(1), 29–36. https://doi.org/10.1109/TEC.2006.889602.

Muljadi, E., Pai, M. A., & Nguyen, T. B. (2009). Transient stability of the grid with a wind power plant. In *2009 IEEE/PES power systems conference and exposition* (pp. 1–7). https://doi.org/10.1109/PSCE.2009.4840030.

Pai, A. (1989). *Energy function analysis for power system stability* (1st ed.). Berlin: Springer. https://doi.org/10.1007/978-1-4613-1635-0.

Samuelsson, O., & Lindahl, S. (2005). On speed stability. *IEEE Transactions on Power Systems*, *20*(2), 1179–1180. https://doi.org/10.1109/TPWRS.2005.846194.

Siemens. (2019). Pss®e 34.0 online documentation

Singh, B., & Singh, S. (2009). Wind power interconnection into the power system: A review of grid code requirements. *The Electricity Journal*, *22*(5), 54–63. https://doi.org/10.1016/j.tej.2009.04.008.

Slootweg, J., & Kling, W. (2003). The impact of large scale wind power generation on power system oscillations. *Electric Power Systems Research*, *67*(1), 9–20. https://doi.org/10.1016/S0378-7796(03)00089-0.

Vittal, E., O'Malley, M., & Keane, A. (2012). Rotor angle stability with high penetrations of wind generation. *IEEE Transactions on Power Systems*, *27*(1), 353–362. https://doi.org/10.1109/TPWRS.2011.2161097.

Vittal, V., & Ayyanar, R. (2013). *Grid integration and dynamic impact of wind energy* (1st ed.). Berlin: Springer. https://doi.org/10.1007/978-1-4419-9323-6.

Yaramasu, V., & Wu, B. (2017). *Model predictive control of wind energy conversion systems* (1st ed.). Piscataway: IEEE Press.